

RESIDUAL GAS BEAM PROFILE MONITOR

John KRIDER

*Fermi National Accelerator Laboratory *, Batavia, Illinois, 60510, USA*

Received 18 January 1989

The design and performance of a beam profile monitor which presents no material to the beam is described. The detector, which has a 75 mm active width, operates from residual gas in the beam vacuum system. It provides 1 mm rms spatial resolution and 1 ms time resolution in a $1 \mu\text{A}$ beam at 10^{-7} Torr. Using a microprocessor based scanning ADC, a sequence of ten profiles can be acquired in as little as 100 ms. The monitor could be applied in other stored or extracted beams where the amount of material seen by the beam must be minimized.

1. Introduction

A non-interactive beam profile monitor has been developed to study betatron stochastic cooling in the Debuncher Ring of the Fermilab Antiproton Source [1]. It is designed to acquire a set of ten profiles of a $1 \mu\text{A}$ beam during the 2 s cooling cycle. Ions from residual gas in the vacuum are drifted onto a microchannel plate assembly, which provides a charge gain of up to 3×10^7 . The charge produced from many primary ions is collected by an array of 48 parallel strips, and it is integrated and digitized with a microprocessor controlled scanning ADC. The monitor was developed from an earlier design, which used microchannel plates with a resistive anode readout and separately processed each ionizing event [2].

2. Design

The monitor consists of independent horizontal and vertical detectors. Fig. 1 is a schematic view of one detector. An electric field perpendicular to the beam causes positive gas ions to drift onto a chevron microchannel plate (MCP) assembly [3]. The sensitive area of the MCP is 75 mm transverse to the beam by 93 mm parallel to the beam. The MCP amplifies the charge signal, which is then collected by a printed circuit array of 48 strips on 1.50 mm centers oriented parallel to the beam.

In order to produce a sufficiently accurate projection

of the beam current density, the charge distribution must be integrated over at least 100 ionizing events. This operation is performed by a Fermilab SWIC (Segmented Wire Ion Chamber) Scanner [4]. The Scanner then digitizes the analog profile and transfers it to the accelerator control system for further analysis and display.

An ion drift field of 35–45 V/mm is maintained in the 120 mm gap between the primary drift electrode on

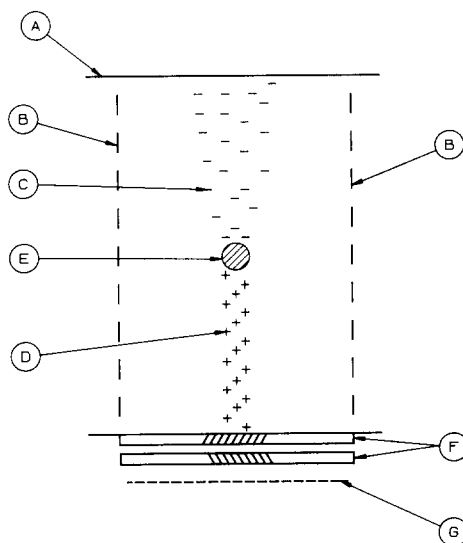


Fig. 1. Cross section of one detector; (A) primary drift electrode, (B) field shaping electrodes, (C) drifting electrons, (D) drifting positive ions, (E) beam, (F) tandem MCPs, (G) anode strips. The drift field is directed vertically downward in this figure.

* Operated by the Universities Research Association, Inc., under contract with the US Department of Energy.

one side of the beam and the MCP on the opposite side of the beam. The field is kept parallel near the sides of the active volume by printed circuit field shaping arrays consisting of nine parallel conductors equally spaced across the gap. The conductors of each array are held at the required potentials by a 100 M Ω voltage divider which is connected across the gap.

The Debuncher vacuum at the location of the monitor is between 1×10^{-7} and 5×10^{-8} Torr. The gas composition is estimated to be 80% hydrogen, 5% water vapor, 5% carbon monoxide, 5% carbon dioxide, and 5% miscellaneous light hydrocarbons. Based on ionization data for the various components of the gas mixture [5], the total specific ionization of the mixture is calculated to be 21 ion pairs per cm at atmospheric pressure. When this is scaled to the monitor vacuum, the probability of a beam particle producing an ion pair is between 1.4×10^{-8} and 2.8×10^{-8} per pass through the detector. Therefore, a beam current of 1 μ A (10^7 circulating particles with a revolution frequency of 590 kHz) produces an ion current of approximately 80 to 160 ions/ms in the detector. Only 60% of the MCP surface is open to accept the incident 2–4 keV positive ions, but within a microchannel the absolute detection efficiency is close to 100% [6]. These factors combine to set a minimum integrating time of about 1 ms to accumulate 100 events from a 1 μ A beam.

The maximum MCP gain is 3×10^7 , but half of the MCP output charge is lost in cable capacitance. The Scanner has a maximum full scale sensitivity of 128 pC per channel. With the MCP and Scanner operating at maximum gain, the minimum programmable Scanner integration time of 1 ms accumulates adequate charge to produce a profile of a 1 μ A beam. Thus, the Scanner charge sensitivity and speed are well matched to the primary ion current from the detector in this application.

The antiproton intensity in the Debuncher is typically in the range of 1 to 10 μ A; however, the current can reach 10 mA during studies with protons. The MCP gain can be adjusted over at least this factor of 10^4 without significantly changing the spatial resolution of the detector.

MCPs suffer permanent gain loss which is proportional to the integrated output charge density [7]. This was studied with a UV light source illuminating a small spot on an MCP. The MCP was operated at maximum gain and produced a peak anode current density of 500 nA/cm². The output pulse height decreased by 16% after an integrated output charge density of 0.074 C/cm². A comparable gain loss would occur in 20 days of continuous operation at maximum gain in the Debuncher. The present detector is powered only a small fraction of the time, and it usually operates with about 100 times lower gain, so radiation damage is not expected to be a serious problem.

3. High voltage system

The high voltage system uses Fermilab designed power supplies [8] and overcurrent protection circuits [9] which limit the anode current. A negative supply sets the MCP gain and the drift field between the MCP and the anodes. A positive supply provides 3 kV to the primary drift electrode. The overcurrent circuit provides a GATE which opens to reduce the MCP voltage by 50% (a gain factor of about 10^3) under the following conditions: (1) at all times except for 10 s during each profile integration; (2) whenever the anode current exceeds a preset limit; and (3) whenever the voltage exceeds the maximum MCP rating. An added benefit of (1) is that the gain is so low during background sampling that beam can be present without affecting the measurement.

4. Readout

The horizontal and vertical detectors are both read out with a single SWIC Scanner, which uses a microprocessor to control 96 analog input channels with 1.0 nF integrating capacitors, a scanning ADC, and memory. The Scanner also contains an algorithm which performs Gaussian fits to the profiles. Integration time and gain are independently programmable from 1 ms to 2 s and from 1 to 2000 respectively.

A Scanner cycle is initiated with a CLEAR pulse, which is followed by a series of up to ten precisely timed START pulses. The CLEAR pulse, which occurs while the MCP high voltage is reduced, causes the Scanner to sample, digitize and store the system background. At the end of background sampling the MCP high voltage is raised, and the independently timed START pulses cause the Scanner to acquire beam profiles. The Scanner subtracts the background from each profile before it is stored. The minimum interval between individual profiles is 10 ms, and the maximum is 10 s. After all of the profiles are stored, the Scanner requires 10 to 15 s to perform Gaussian fits and generate a video output of the profiles and fit parameters. The data can also be transmitted to the accelerator control system for more sophisticated analysis and display.

5. Spatial resolution

Spatial resolution is determined by a number of factors: (1) transverse growth of the primary ion cloud; (2) gain variations within the MCP; (3) gain variation from one Scanner channel to another; (4) transverse growth of the electron cloud between the two MCP

layers, and between the second MCP and the anodes; and (5) the Gaussian fitting routine.

When a profile is produced from positive ions, most of the ion drift error is caused by nonuniformities in the drift field. Computer modelling indicates that this degrades the resolution by up to 0.5 mm rms.

The MCP gain was observed to vary by less than 10% over the entire active area, when it was scanned with a UV light beam. Channel to channel gain variation in the Scanner is less than 5%. These two effects contribute a total of about 0.2 mm rms to the overall detector resolution.

The gap between the two MCPs is 0.25 mm and has an accelerating potential of about 1 V. The gap between the output of the MCPs and the anode strips is 1.5 mm and has an accelerating potential in the range of 125–250 V. Calculations show that these gaps add 0.4 mm rms to the profile width measurements [10].

The width and mean of profiles are calculated with a Gaussian fitting routine. For Gaussian beams these parameters have a calculation error of about 0.1 mm rms. For non-Gaussian beams the fitting error can be considerably larger, and a different fitting routine may be required. Debuncher beam profiles are typically nearly Gaussian.

Combining all of the preceding factors in quadrature yields a predicted resolution of 0.7 mm rms from positive ions. The narrowest beam actually measured by the monitor sets an upper limit on the true spatial resolution. The monitor measured that beam to be 1.04 mm rms.

When the drift field polarity was reversed to drift primary electrons to the MCP, the MCP output charge was observed to be 8 times larger than the charge produced from positive ions. The increased signal is believed to be produced from primary electrons striking the MCP surface between microchannels. The drift field directs some of the secondary and tertiary electrons from these surface interactions into the microchannels as additional signal. In contrast, the field polarity which drifts positive ions toward the MCP repels these secondary electrons from the MCP.

There is a significant loss of spatial resolution in profiles produced from primary electrons. One contribution is the above described splash of secondary electrons at the MCP surface. Also, the energy transfer to the primary electron at ionization is typically much larger than the energy transfer to the positive ion [11]. The component of this energy which is transverse to the drift field shifts the electron's point of arrival at the MCP. For example, 2 eV of transverse energy produces a 1 mm shift over a 60 mm drift. A beam with relatively sharp edges was used to measure resolution from primary electrons. The positive ion profile measured the beam intensity to increase from 10% to 90% of maximum in 4.5 mm, while the profile using electrons meas-

ured 8.0 mm. The resolution with positive ions was previously measured to be 1 mm rms, so the resolution with electrons is inferred to be 4.0 mm rms.

A UV window mounted in the wall of the monitor vacuum chamber allows a collimated UV light source to project a 1 mm diameter spot onto the MCP surface. This has been a useful diagnostic tool on several occasions, since the monitor is located in an area which is not accessible when the Antiproton Source is operating. Since the UV spot is comparable in size to the overall resolution of the monitor, it provides an accurate test of all of the system, except the production and drift of the primary ions.

6. Beam profiles of stochastic cooling

Fig. 2 shows the control system display of a set of ten horizontal and vertical profiles taken during the stochastic cooling of antiprotons. The profile data appear as histograms, and the superposed smooth curves are the Gaussian fits. The profiles were taken at 200 ms intervals with an integration time of 133 ms for each profile. The profiles show graphic evidence of the reduction in beam size achieved by the cooling system.

Fig. 3 displays the rms width, charge integral and mean as a function of scan number for the profiles of fig. 2. The width decreased to 0.53 of its initial value in the horizontal plane and to 0.52 in the vertical plane. The integrals both decreased to about 0.6 of their initial values, indicating a loss of 40% of the beam during this cooling cycle. In a separate set of measurements during normal machine operation, there was not significant beam loss during cooling, and the integrals remained constant to within 5%. The mean positions, or beam center, changed by less than 1 mm during the scans.

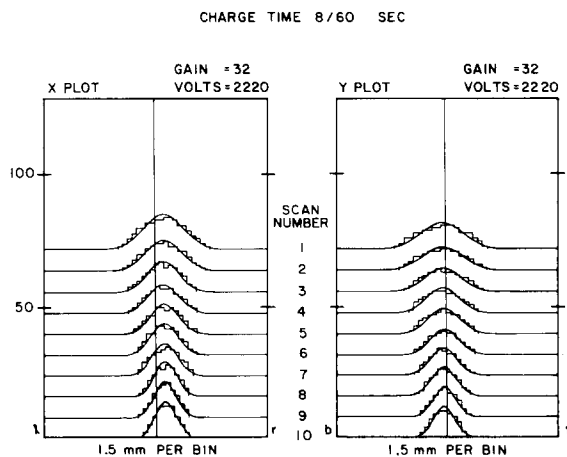


Fig. 2. Set of beam profiles taken during stochastic cooling.

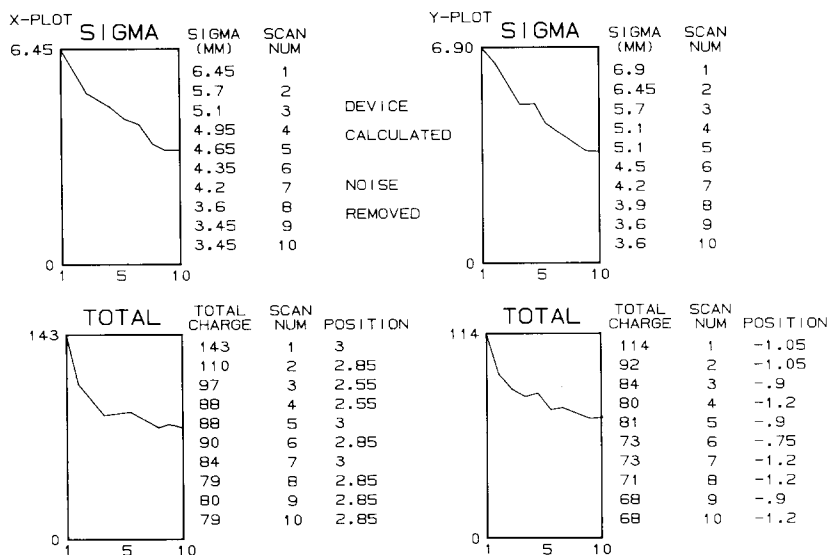


Fig. 3. Gaussian fit parameters for the profiles of fig. 2.

There are no other devices which directly measure beam profiles in the Debuncher; however, a beam Schottky noise spectrum monitor provides a signal which is proportional to the width of the beam at this location in the ring. For one cooling cycle the width measured by the profile monitor decreased by 39%, from 6.60 mm to 4.05 mm. The Schottky signal indicated a decrease of 41% during the same cycle, showing good agreement between the two devices.

7. Summary

In summary, a beam profile monitor which introduces essentially no material into the beam has been described. The detector has a spatial resolution of 1 mm and time resolution of 1 ms, and it can produce a sequence of ten profiles at a rate of 100 Hz. It has operated in beams ranging in intensity from 1 μ A to 10 mA. When time resolution is not crucial, the range of the monitor can be extended to lower beam intensity by increasing the profile integration time. The range could also be extended by introducing a small amount of additional gas into the beam in the vicinity of the monitor, when a set of profiles is being taken. Once calibrated, the profile integrals provide a useful beam intensity monitor.

Acknowledgements

The author would like to recognize several people for their contributions to the project. Bill Kells and Jerry Rosen did most of the early design work, and they generously shared what they had learned. Don Poll performed the mechanical and electrical assembly, and Alan Riddiford provided the control system software. I would also like to thank Stephen Pordes for his assistance in editing this article.

References

- [1] J. Peoples, IEEE Trans. Nucl. Sci. NS-30 (1983) 1970.
- [2] T. Hardek, W. Kells and H. Lai, IEEE Trans. Nucl. Sci. NS-28 (1981) 2386.
- [3] Model 3810 Chevron CEMA, Galileo Electro-Optics Corp., Sturbridge, MA, USA.
- [4] B. Higgins, Fermilab TM-868-A (1983).
- [5] F. Sauli, CERN Report 77-09 (1977).
- [6] E.A. Kurz, American Laboratory (March, 1979).
- [7] J. L. Wisa, Nucl. Instr. and Meth. 162 (1979) 587.
- [8] Droege MWPC High Voltage Supply, Fermilab Model ES-7109 (negative polarity) and Model ES-7125 (positive polarity).
- [9] J. Krider, Debuncher Profile Monitor Users Guide, Fermilab Antiproton Source Internal Note.
- [10] J.L. Wisa, P.R. Henkel and R.L. Roy, Nucl. Instr. and Meth. 48 (1975) 1217.
- [11] R.C. Fernow, Introduction to Experimental Particle Physics (Cambridge University Press, 1986) section 2.1.